

# Evaluation of hydroxyl content in commercial X-cut LiNbO<sub>3</sub> wafers for optical waveguide devices

**Hirotooshi Nagata**

Sumitomo Osaka Cement Co., Ltd.  
New Technology Research Laboratories  
Optoelectronics Research Division  
585 Toyotomi-cho  
Funabashi-shi, Chiba 274 8601  
Japan

**Abstract.** Usually the quality of commercial LiNbO<sub>3</sub> (LN) wafers is checked by their crystalline homogeneity. In X cut wafers, which are labeled for optical waveguide applications, however, the existence of a significant change in the hydroxyl content along the polarized Z axis is found by Fourier transform IR (FTIR) spectrometry, although a corresponding inhomogeneity was not observed about the lattice parameters, the Li and Nb contents, and the optical birefringence parameters. Such a difference in hydroxyl content might influence quality and stability of the obtained waveguides, and one should consider this before designing waveguide devices and fabrication processes. © 1998 Society of Photo-Optical Instrumentation Engineers. [S0091-3286(98)01905-9]

Subject terms: LiNbO<sub>3</sub> hydroxyl ions; wafer; waveguide devices; process inspection.

Paper37077 received July 22, 1997; revised manuscript received Nov. 20, 1997; accepted for publication Nov. 20, 1997. This paper is a revision of a paper presented at the SPIE Conference on Optoelectronic Integrated Circuits, February 1997, San Jose, CA, and published in Proc. SPIE Vol. 3006 (1997).

## 1 Introduction

In 1968 Smith et al. studied hydroxyl contamination in a LiNbO<sub>3</sub> (LN) crystal, and an optically induced refractive index inhomogeneity was shown to be reduced for the LN containing larger amounts of hydroxyl ions.<sup>1</sup> They also found that the hydroxyl content changed along the polarized Z axis of the crystal, with a higher content near the external anode side, while it was lower near the cathode side.<sup>1</sup> They speculated that the reason for this phenomenon was that during the polarization process, protons were produced around the anode from water vapor in the air and were injected electrically into the LN crystal.<sup>1</sup> Another possible explanation is that hydroxyl ions in the LN crystal were diffused toward the anode side by a strong electric field during the polarization process. Therefore, the hydroxyl content in the Z cut wafers differed, depending on the position in the ingot from which the wafer was sliced.<sup>1,2</sup> In the X cut wafer, as described in this paper, hydroxyl content changes along the Z axis even in the same wafer.

The influence of hydroxyl contamination in LN optical waveguide characteristics was recently reported by Koide et al.,<sup>3,4</sup> who investigated the generation of the surface layer with an anomalous optical refractive index due to a heat treatment near 1000°C, and concluded that thermal diffusion of the hydroxyl ions through the wafer surface led to the anomaly in the refractive index at the surface.<sup>4</sup> The magnitude of the anomaly depended on both the initial content of hydroxyl ions in the wafers and the moisture content in the annealing atmosphere.<sup>4</sup> Previously, it was found that a thermal reconstruction of surface morphology in the LN wafer was also affected by hydroxyl content in the wafer.<sup>5-7</sup> Furthermore, drift phenomena in the optical out-

put signal of LN optical modulators were also known to depend on the hydroxyl content in the LN substrates.<sup>1,8,9</sup>

The X cut LN device fabrication experience has shown that unevenness in optical propagation characteristics is frequently found, even in devices made from the same wafer. This may be due to inhomogeneous titanium-indiffused waveguides being formed. Also, the repeatability of the dc-drift phenomena seems to be inferior for X cut optical intensity modulators rather than for Z cut modulators.

From these results, the fluctuation in hydroxyl content of the LN wafers was thought to strongly affect the optical characteristics of the waveguides obtained by a titanium diffusion at high temperatures or a proton exchange treatment. Actually, I believe the present fabrication yields of LN waveguide devices is not high enough.<sup>10</sup> Usually, the only quality assurance measures used for optical quality LN wafers are x-ray topography, Curie temperature, and chemical composition. In addition to such conventional inspection, I propose the necessity for evaluation of the hydroxyl content in the wafers to improve the yield of quality waveguide devices. Because hydroxyl ions are inevitably included in the crystal, a postannealing of the wafers in a dry atmosphere, as reported by Koide et al.,<sup>3</sup> is considered to be a practical method to homogenize the hydroxyl contents.

In this paper, I mainly present the results of hydroxyl content measurement of certain commercial wafers, which were labeled for optical waveguide applications.

## 2 Hydroxyl Content Distribution in X Cut Wafers

Because excess protons are interstitially trapped in oxygen planes of the LN crystal structure, the resulting hydroxyl

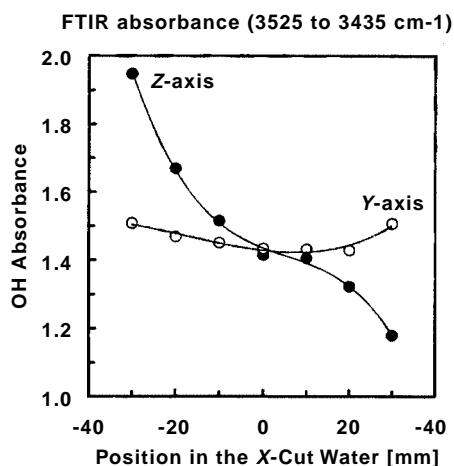


**Fig. 1** Hydroxyl content distribution on the X cut wafer along the Z axis (solid circles) and the Y axis (open circles).

bonding ( $\text{O-H}$ ) is excited<sup>11</sup> by a lightwave vibrating (polarized) normal to the Z axis of the LN. Using this phenomenon, the amount of the hydroxyl content in the X cut LN wafers was measured by a Fourier transform IR (FTIR) spectrometer accompanied by a polarizer placed between the light source and the wafer. When the polarizer is set normal to the Z axis, peaks due to an OH stretching mode appear between 3525 and 3435  $\text{cm}^{-1}$ , depending on the difference in distance from the corresponding proton to the nearest oxygen.<sup>12,13</sup> No peak was observed for the incident lightwave polarized parallel to the Z axis.

The measurement was carried out for several commercial X cut wafers sliced from two different LN crystal ingots. The diameter and the thickness of the wafers were 76.2 and 0.5 mm, respectively. Similar results were obtained for all samples, as shown in Fig. 1, in which the magnitude of the OH absorbance measured by the FTIR spectrometer is plotted as a function of the distance from the wafer center. The magnitude of the OH absorbance was calculated<sup>14</sup> from the area for the OH-induced peaks between 3525 and 3435  $\text{cm}^{-1}$ . In Fig. 1, the solid circles show the position dependency of the OH absorbance, i.e., the hydroxyl contents along the Z axis on the X cut wafer, while the open circles represent the data along the Y axis. As seen, the hydroxyl content changes greatly along the Z axis, and the -Z end of the wafer contained twice as many hydroxyl ions as the +Z end. Because the -Z end was connected to the external anode during the crystal ingot polarization process, the observed results were consistent with the data from Smith et al. for a cross section of the Z axial grown ingot.<sup>1</sup> The distribution of the hydroxyl content along the Y axis was relatively homogeneous.

The X cut LN waveguide devices, such as Mach-Zehnder intensity modulators and polarization scramblers, are generally designed to have waveguides parallel to the Y axis and to apply the electric field along the Z axis. Therefore, although the device chips were cut from the same wafer, Fig. 1 indicates that the hydroxyl content was different for different locations on the wafer. Although the influence of the hydroxyl content on the fabricated devices has not yet been clarified, there is a possibility that the diffil-

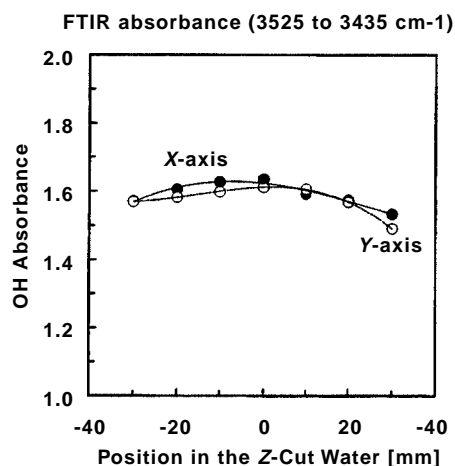


**Fig. 2** Hydroxyl content distribution on the Z cut wafer along the X axis (solid circles) and the Y axis (open circles).

sion process for waveguide formation is affected by the hydroxyl ions, especially when the waveguides are prepared in a region of the wafer beyond  $\pm 20$  mm from the wafer center.

To compare the X cut wafers, the hydroxyl content in Z cut wafers was similarly evaluated, as shown in Fig. 2. The distribution of the hydroxyl content was measured to be almost homogeneous in the wafer. The absolute value of the OH absorbance for different wafers, which were sliced from neighboring positions in the ingot, was similar. The difference in the hydroxyl content dependent on position in the X cut wafer was also checked by thermal desorption spectrometry (TDS). For the analysis, two square-shaped samples 6 Å~6 mm in size were cut from a position +30 and -30 mm from the wafer center along the Z axis, respectively, and were heated in vacuum (about 5 Å~ $10^{-7}$  Pa) up to 1000°C with a heating rate of 60 K/min. During the heating, gases evaporated from the sample were detected by the mass analyzers tuned at 2 ( $\text{H}_2$ ), 17 (OH), 18 ( $\text{H}_2\text{O}$ ). The TDS results for mass numbers 2 and 18 are shown in Figs. 3(a) and 3(b), respectively, in which the result for the +30 sample is shown by a solid curve and the -30 sample by a dotted curve. The results for mass number 17 were similar with those for mass number 18. The difference in the spectra for mass number 2 was not clear between the two samples, and a rapid increase beyond 900 Å seemed to partially include a background signal due to the equipment. However, the amount of desorption of the  $\text{H}_2\text{O}$  species (mass number 18) was significantly larger for the -30 sample over 600°C. The  $\text{H}_2\text{O}$  species detected at high temperatures were considered to be caused by the hydroxyl ions in the LN crystal, rather than surface contamination. The relative peak intensity for mass number 18 of the -30 sample was 1.7 times stronger than the +30 sample, supporting the results by FTIR spectrometer measurements in Fig. 1.

Figures 4(a) and 4(b) are optical micrographs for the +30 and -30 samples, respectively, after the TDS measurement, i.e., annealing in the vacuum. For the -30 sample, which contained a larger amount of the hydroxyl ions, the generation of domains giving a clear optical con-

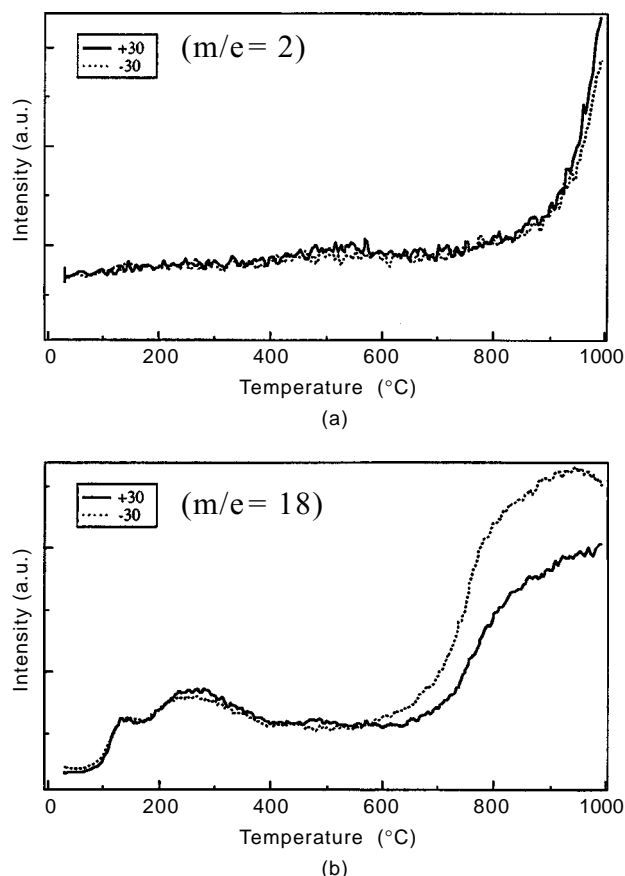


**Fig.3** Temperature dependency of the amounts of (a) H<sub>2</sub> (mass number 2) and (b) H<sub>2</sub>O (mass number 18) evaporated from the LN samples during the vacuum annealing i.e., TDS analyses. The solid and dotted curves denote the results for samples taken from positions +30 and -30mm from the center of the X cut LN wafer, respectively.

trast was observed, while no specific contrast was observed for the annealed +30 sample and the -30 before annealing. These annealed samples were powdered and analyzed by x-ray diffractometry, but no additional crystalline phase was detected, giving no information about the anomalous structure shown in Fig. 4(b).

### 3 Structural Homogeneity of X Cut Wafers

As described, the hydroxyl content in the commercial X cut LN wafers was inhomogeneous along the Z axis. On the other hand, the quality of the commercial LN wafers were checked with respect to their structural homogeneity by chemical analyses, x-ray topography, etc. Here, the X cut wafers, which were confirmed to have inhomogeneous hydroxyl content, were evaluated in terms of their structural parameters, such as the Li/Nb chemical composition, the crystal structure, the existence of crystal defects, and the optical birefringence. No correspondence was found between the measured parameters and the distribution of hydroxyl content, suggesting the difficulty in inspecting the LN wafer quality by only conventional methods.

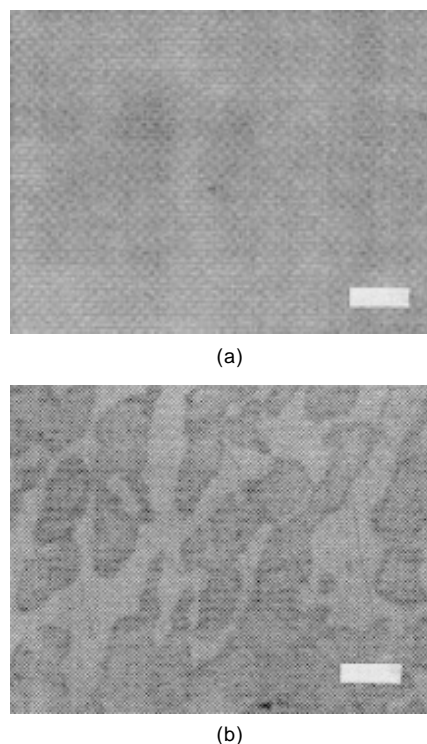


**Fig. 4** Optical micrographs for the samples after the TDS analyses (vacuum annealing up to 1000°C): samples taken from the positions (a) +30mm and (b) -30mm from the center of the X cut LN wafer. The length of bars in the photos denotes 100 µm.

### 3.1 Chemical Composition

Concentrations of Li and Nb were measured by atomic absorption spectrometry (AAS) and by inductively coupled plasma (ICP) spectrometry, respectively. To check the distribution of the composition in the wafer, before the measurement, the wafer was cut into 10Å~10 mm squares and each one was dissolved completely in HF for the analyses. Figures 5(a), 5(b), and 5(c) show the measured Li contents in weight percent, Nb contents in weight percent, and calculated Li/Nb atomic ratio, respectively. The position dependency of the chemical composition on the wafer is represented by solid circles for the Z axial direction and by open circles for the Y axial direction. Because of difficulties in the Li concentration measurements, the obtained Li content was larger than the value expected<sup>15,16</sup> for the congruent composition of the LN. Further, the data for both elements were scattered, but at least the distribution profile of the Li and Nb in the wafer was independent of that of the hydroxyl content.

### 3.2 Crystallinity

A change in the Li/Nb atomic ratio in the LN can be checked by crystal lattice lengths: the a (X) and c (Z) axial lengths expand with a decrease of the Li concentration. Figures 6(a) and 6(b) show a change of the a and c axial lengths, respectively, along the Z axis of the other X cut wafer, measured by conventional powder x-ray diffractometry. The axial lengths were calculated using diffraction peaks appearing between 2θ=48 to 105 deg. Considering

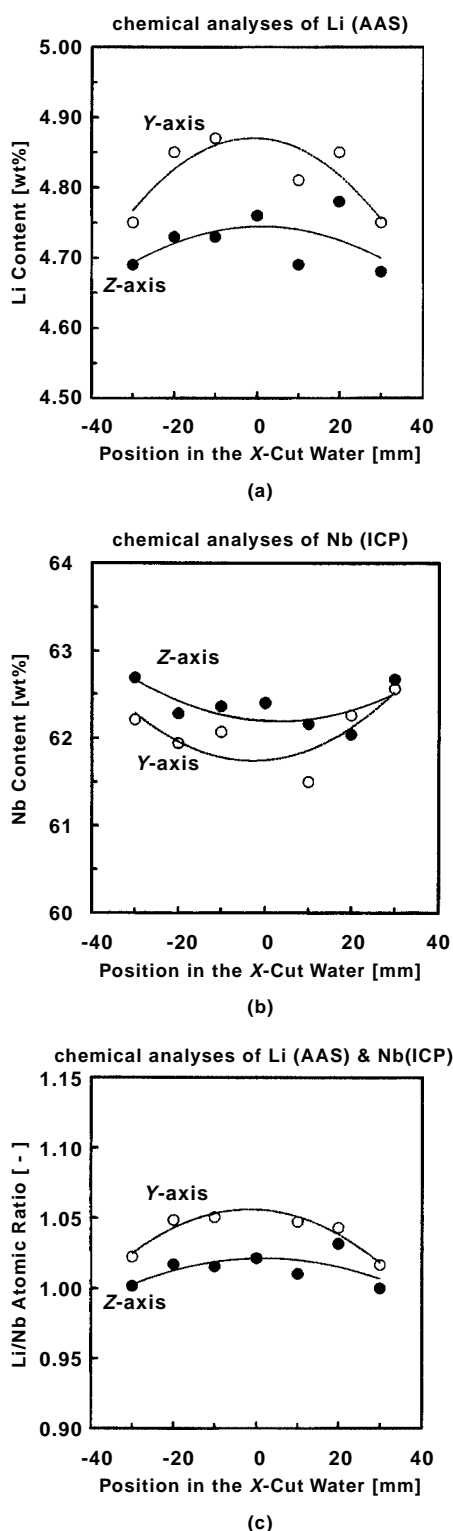


**Fig. 5** (a) Li content in weight percent, (b) Nb content in weight percent, and (c) Li/Nb atomic ratio depending on the position along the Z axis (solid circles) and the Y axis (open circles) in the same X cut wafer.

the magnitude of the measurement errors and the fact that the lattice lengths were almost identical in the wafer, suggests that the measurement of the lattice parameters did not detect the anomaly in the hydroxyl contents.

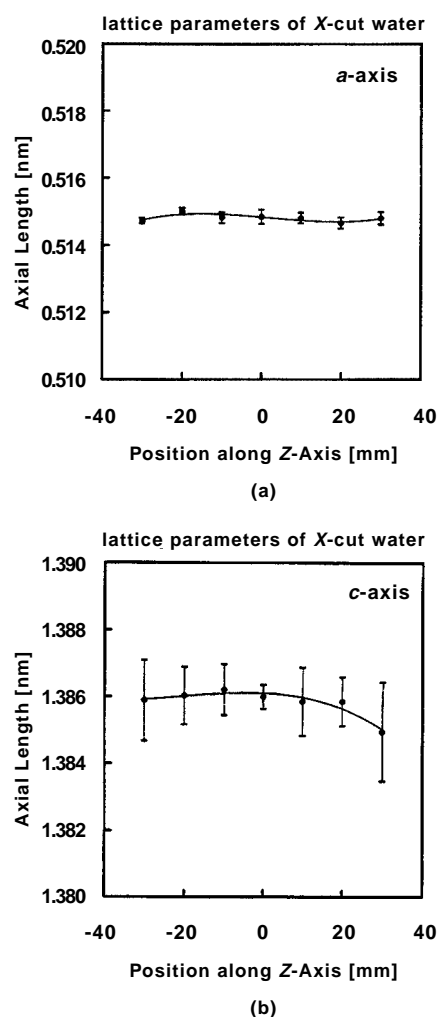


**Fig. 6** Position dependency along the Z axis of (a) a axial length and (b) c axial length of the X cut wafer.

The other X cut LN wafers were also evaluated by x-ray diffraction topography using a Lang camera with a Mo  $K_{\alpha 1}$  line at 50 kV ([006] axial transmission). The results are shown in Figs. 7(a) and 8(a), for two wafers sliced from different LN ingots, in which the horizontal direction of the images corresponds to the Z axis of the wafer. For the wafer of Fig. 7(a), the density of dislocation-type defects was estimated to be of the order of  $10^3/\text{cm}^2$ , and they seemed to scatter homogeneously throughout the wafer independent of the distribution of the hydroxyl content. Although the wafer of Fig. 8(a) included a large defect near the center of the wafer, the x-ray topographic evaluation did not detect a fluctuation in the hydroxyl content of the wafer.

### 3.3 Optical Birefringence

Finally, a planar distribution of optical birefringence was evaluated for the X-cut wafers, but similarly it provided information corresponding only to the crystal defects, not to the hydroxyl content. The birefringence of LN wafers in Figs. 7(a) and 8(a) was measured at ordinary room temperatures by an optical heterodyne method using a commer-

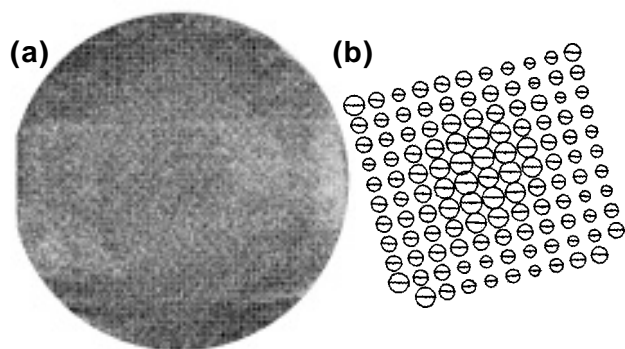


**Fig. 7** (a) The x-ray diffraction topography image and (b) the planar distribution image of birefringence parameters both measured for the same 3-in.-diam X cut LN wafer. The birefringence parameters were measured in a 50 × 50mm area of the wafer. In (b), the size of the circle and the bar in circles denote, respectively, the magnitude of the optical phase retardation and the direction of the optical main axis. The magnification of the images in (a) and (b) are similar.

cial machine (Uniopt Co. Ltd. Model ABR-10A) equipped with a Zeeman laser ( $\lambda = 632.8\text{nm}$  and  $d = 0.75\text{mm}$  beam) and an x-y sample scanner.

Figures 7(a) and 7(b) show the x-ray topography images and the planar distributions of the birefringence measured for the same wafer. The birefringence was measured at 5-mm intervals in the 50- × 50-mm square area of the wafer, and in Fig. 7(b) the magnitude of each birefringence was displayed using circles of a corresponding size. The size of these circles denotes the phase retardation induced by the LN in the two perpendicularly polarized light beams. Further, these retardation values were reduced to a unit of length by multiplying the beam wavelength. In the case of Fig. 7(b), the magnitude of the reduced retardation varied from 127.9 to 284.9nm in the 50- × 50-mm area, and the average value and 3  $\sigma$  value ( $\sigma$  = standard deviations) were 193.3 and 113.5nm, respectively. As is seen, the distribution of the retardation values was almost homogeneous in the wafer, except for the tendency for the center of the wafer to show slightly larger retardation. The reason for such a tendency must be clarified, although the existence of

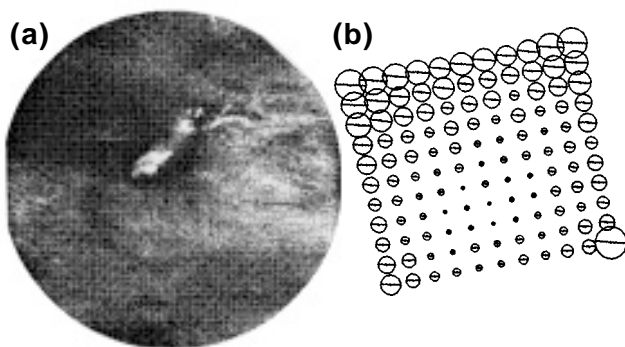


**Fig. 8** (a) The x-ray diffraction topography image and (b) the planar distribution image of birefringence parameters both measured for the same 3-in.-diam X cut LN wafer. This wafer had significant crystalline defects.

a slight change in the wafer thickness from the center to the edge possibly affected the results.

In Fig. 7(b), the direction of the main optical axis measured at each point was also displayed by a diametric line in the circle. Because the LN wafer was polarized to have a single domain structure, the optical axis was observed to be well aligned. The preceding birefringence measurement results indicate the homogeneous quality of the wafer and are consistent with the results from the x-ray topography of Fig. 7(a).

On the other hand, as shown in Figs. 8(a) and 8(b), the results measured for another inferior wafer revealed anomalies in the optical retardation values around significant crystalline defects, although the optical axis aligned even in the defects. The measured retardation was distributed primarily from 19.6 to 210.5nm in the 50- × 50-mm area; average = 83.0nm and 3  $\sigma$  = 136.8nm. The measurement of the planar distribution for the birefringence parameters was at least thought to be a suitable method for the evaluation of the crystalline quality in the LN wafers. The wafer in Fig. 8, for instance, should be rejected from the device fabrication line to prevent instability in device performance.

#### 4 Conclusions

Hydroxyl ions are inevitably included in the LN crystals, and their concentration was found to change along the  $Z$  axis in  $X$  cut wafers. In this regard, there is a possibility that such a hydroxyl content difference may lead to unevenness in the diffusion behavior and the obtained optical waveguide characteristics on the same wafer. However, conventional wafer inspection methods could not reveal such an anomaly in the hydroxyl content.

#### 5 Additional Comments

Although the crystalline quality of the LN wafers has been greatly improved during the last 10 years, the criteria for wafer screening are not yet clear. Actually, with an increasing market for LN devices, the problem of inferior fabrication yield sometimes arises for certain LN devices. I consider the uneven distribution of the hydroxyl contents and crystalline defects in the wafer one of origins of the problem. This paper reveals the existence of such unevenness even in commercial wafers for optical applications. At this time, however, I can not show the quantitative parameters for the screening of LN wafers in relation to the absolute hydroxyl content and the degree of birefringence homogeneity, because any allowance for unevenness in device characteristics depends on the device type. For instance, it is found that the optical output characteristics of LN polarization modulators are strongly affected by the fabrication repeatability of the Ti-indiffused waveguides, and influence of both the hydroxyl contents and the crystalline defects in the wafer must be considered. On the other hand, the stability of intensity modulators depends partially on the hydroxyl contents in the wafer via the dc drift phenomena.

#### Acknowledgments

This study was partially supported by Special Coordination Funds for Promoting Science and Technology for fundamental research on new materials of function-harmonized

xides, from the Japanese Science and Technology Agency, to whom the author is deeply indebted. The author also gratefully thanks Dr. Minowa and Mr. Totani of Sumitomo Osaka Cement for helpful discussions, Chuken Consultant Co. Ltd. for the ASS and ICP spectrometry measurements, Toray Research Center Inc. for the TDS analyses and the x-ray topography observation, and Uniopt Co. Ltd. for the birefringence measurements.

## Reference

1. R. G. Smith, D. B. Fraser, R. T. Denton, and T. C. Rich, "Correlation of reduction in optically induced refractive-index inhomogeneity with OH content in  $\text{LiNbO}_3$  and  $\text{LiNbO}_3$ ," *J. Appl. Phys.* **39**(10), 4600-4602 (1968).
2. H. Nagata and J. Ichikawa, "Progress and problems in reliability of Ti:LiNbO<sub>3</sub> optical intensity modulators," *Opt. Eng.* **34**(11), 3284-3293 (1995).
3. A. Koide, H. Shimizu, and T. Saito, "Prevention of thermal degradations by using dehydrated LiNbO<sub>3</sub> crystal," *Jpn. J. Appl. Phys.* **33**(7A), L957-L958 (1994).
4. A. Koide, H. Shimizu, and T. Saito, "Main cause of surface waveguides formed under LiNbO<sub>3</sub> crystal surface during thermal treatment," *Jpn. J. Appl. Phys.* **36**(1A), 239-242 (1997).
5. H. Nagata and S. Kaori, "Surface steps observed in a dry annealed z-cut LiNbO<sub>3</sub> substrate," *Jpn. J. Appl. Phys.* **35**(7A), 4040-4041 (1996).
6. H. Nagata, T. Sakamoto, H. Honda, J. Ichikawa, E. M. Haga, K. Shima, and N. Haga, "Reduced thermal decomposition of OH-free LiNbO<sub>3</sub> substrates even in a dry gas atmosphere," *J. Mater. Res.* **11**(8), 2085-2091 (1996).
7. H. Nagata, K. Shima, and J. Ichikawa, "Effect of hydroxyl content on thermally induced change in surface morphology of lithium niobate (0001) substrates," *J. Am. Ceram. Soc.* **80**(5), 1203-1207 (1997).
8. H. Nagata, J. Ichikawa, M. Kobayashi, J. Hidaka, H. Honda, K. Kiuchi, and T. Sukanlata, "Possibility of dc drift reduction of Ti:LiNbO<sub>3</sub> modulators via dry O<sub>2</sub> annealing process," *Appl. Phys. Lett.* **64**(10), 1180-1182 (1994).
9. H. Nagata, J. Ichikawa, N. Mitsugi, T. Sakamoto, T. Shinriki, H. Honda, and M. Kobayashi, "Improved long-term dc drift in OH-reduced lithium niobate optical intensity modulators," *Eng. Lab. NOTES OPT. Photon. News* **7**(5), (1996).
10. H. Nagata, N. Mitsugi, J. Ichikawa and J. Minowa, "Materials reliability for high-speed lithium niobate modulators," *Proc. SPIE* **3006**, 301-313 (1997).
11. J. R. Herrington, B. Dischler, A. Rauber, and J. Schneider, "An optical study of the stretching absorption band near 3 microns from OH- defects in LiNbO<sub>3</sub>," *Solid State Commun.* **12**, 351-354 (1973).
12. L. Kovacs, M. Wohlecke, A. Jovanovic, K. Polgar, and S. Kapphan, "Infrared absorption study of the OH vibrational band in LiNbO<sub>3</sub> crystals," *J. Phys. Chem. Solids* **52**(6), 797-803 (1991).
13. O. F. Schirmer, O. Thiemann, and M. Wohlecke, "Defects in LiNbO<sub>3</sub> - I. experimental aspects," *J. Phys. Chem Solids* **52**(1), 185-200 (1991).
14. W. Bollmann and H.-J. Stohr, "Incorporation and mobility of OH-ions in LiNbO<sub>3</sub> crystals," *Phys. Status Solidi A* **39**, 477-484 (1977).
15. W. A. Tiller and S. Uda, "Intrinsic LiNbO<sub>3</sub> melt species partitioning at the congruent melt composition," *J. Crystal Growth* **129**, 328-340 (1993).
16. P. F. Bordui, R. G. Norwood, C. D. Bird, and G. D. Calvert, "Composition uniformity in growth and poling of large-diameter lithium niobate crystals," *J. Crystal Growth* **113**, 61-68 (1991).



**Hirotohi Nagata** received his BS in inorganic materials engineering from the Nagoya Institute of Technology in 1984 and his DEng in materials science from Tokyo Institute of Technology in 1992 for the study of epitaxial film growth of oxide materials. In 1984 he joined New Technology Research Laboratories of Sumitomo Osaka Cement Co. Ltd., engaged in research and development of ceramics materials and films. Since 1992 he has been investigating reliability and quality issues of LiNbO<sub>3</sub>-based optical waveguide devices at the Optoelectronics Research Division of Sumitomo. From 1995 to 1997, he was a part-time instructor with Yokohama National University. He is a member of the Optical Society of America and the Materials Research Society.